Journal of Solid State Chemistry 184 (2011) 1279–1285

Contents lists available at ScienceDirect

Journal of Solid State Chemistry

journal homepage: www.elsevier.com/locate/jssc

A series of M–M' heterometallic coordination polymers: syntheses, structures and surface photoelectric properties (M=Ni/Co, M'=Cd/Zn)

Lei Li [a], Shu-Yun Niu [a,*], Jing Jin [a], Qin Meng [a], Yu-Xian Chi [a], Yong-Heng Xing [a], Guang-Ning Zhang [b]

[a] School of Chemistry and Chemical Engineering, Liaoning Normal University, Dalian 116029, PR China
[b] Institute of Chemistry for Functionalized Materials, Liaoning Normal University, Dalian 116029, PR China

ARTICLE INFO

Article history:
Received 14 January 2011
Received in revised form
17 March 2011
Accepted 27 March 2011
Available online 2 April 2011

Keywords:
Heterometallic coordination polymer
Synthesis
Structure
Surface photovoltage spectroscopy

ABSTRACT

Four new heterometallic polymers, $[NiCd(mal)_2(H_2O)_2]n\cdot 2nH_2O$ **1**, $[NiZn_2(Hcit)_2(H_2O)_2]n$ **2**, $[CoCd_2(Hcit)_2(H_2O)_2]n$ **3**, $[CoZn_2(Hcit)_2(H_2O)_2]n$ **4** (H_2mal=malonic acid, H_4cit=citric acid) were synthesized and characterized. The photoelectric properties of the polymers were discussed by the surface photovoltage spectroscopy (SPS). The structural analyses indicate **1** is a Ni–Cd heterometallic polymer with 3D structure bridged by the mal^{2-} group. **2**–**4** are all heterometallic polymers with 2D structures bridged by the $Hcit^{3-}$ group. The results of SPS for the four polymers reveal that there are wide photovoltage response bands in the range of 300–800 nm, which indicates that they all possess photoelectric conversion properties. By the introduction of the other metals, the SPS of heterometallic polymers are broadened obviously than the SPS of monometallic complexes. Moreover, the relationships between SPS and UV–Vis absorption spectra have been discussed.

1. Introduction

As a major branch of the coordination chemistry, heterometallic complexes have been given extensive attentions [1–5]. The simultaneous presences of heterometallic centers in the complexes could lead to not only fascinated structures but also novel properties, such as magnetism, catalysis, electrochemistry, optics, etc. [6–9]. There have been a number of investigations on heterometallic complexes and most were concentrated on 3*d*–3*d*' [10], 3*d*–4*d* [11], 3*d*–5*d* [12], 3*d*–4*f* [13], 4*d*–4*f* [14], etc. For example, Timco and Winpemmy reported a series of Cr–3*d*' heterometallic complexes and found that there were anti-ferromagnetic exchanges in the molecules [15,16]. Niu reported a series of d^{10}–4*f* complexes and discussed the influences of d^{10} metal on NIR luminescence of 4*f* blocks [17,18]. A large number of heterometallic polymers bridged by CN^- and SCN^-groups were reported with ferromagnetic coupling and ferroelectricity in the most of them [19–21]. The magnetic researches of heterometallic complexes indicate that the introduction of heterometals develops the fashion and channels of electron transitions, on the basis of which the ferromagnetic materials may be designed [22]. But the reports about photoelectric properties are rare. As a high sensitive detection tool, surface photovoltage spectroscopy (SPS) has been applied widely to the detection of electron transitions on the surface and interface [23–26]. SPS not only relates to the charge transition under light inducement but also reflects the separation and transfer of photogenerated charges directly [27–30]. At present, the research of photoelectric properties with SPS is concentrated on the complexes with macrocyclic ligands, such as porphyrin and phthalocyanine [31–33]. The reports about photoelectric properties with transitional metal complexes are rare [34–39].

With malonic acid and citric acid as bridging ligands, four heterometallic polymers, Ni(II)–Cd(II), Ni(II)–Zn(II), Co(II)–Cd(II), and Co(II)–Zn(II), were synthesized and their structures were determined by single-crystal X-ray diffraction. The influences of introduction of the heterometal on the SPS were discussed emphatically.

2. Experimental section

2.1. Materials and apparatus

All chemicals were of A.R. grade without further purification. Single-crystal X-ray diffraction data were collected with Smart 1000 APEX II diffractometer equipment. IR spectra were recorded as KBr pellets with a JASCO FT-IR/480 spectrophotometer and UV–Vis diffuse reflectance spectra were recorded with a JASCO V–570 UV–Vis–NIR spectrophotometer. The elemental analyses were detected on a PE-240 C Analyzer and TLASMA–II ICP instrument. The X-ray powder diffraction (XRD) data of complex **1** was collected on a Bruker Advance-D8 diffractometer and those of **2**–**4** were collected on a D/Max 2400 diffractometer. The thermal gravimetric (TG) analyses were carried out in the temperature

* Corresponding author. Fax: +86 411 82156832.
E-mail address: syniu@sohu.com (S.-Y. Niu).

0022-4596/$ - see front matter © 2011 Elsevier Inc. All rights reserved.
doi:10.1016/j.jssc.2011.03.046

range of 30–1000 °C on a Pyris diffractometer. SPS were performed on a home-built surface photovoltage spectrophotometer.

2.2. Preparations of the complexes

2.2.1. Preparation of $[NiCd(mal)_2(H_2O)_2]_n \cdot 2nH_2O$ **1**

$NiCl_2 \cdot 6H_2O$ (0.12 g, 0.5 mmol) and $CdCl_2 \cdot 2.5H_2O$ (0.11 g, 0.5 mmol) were dissolved in deioned water (15 mL) and then the solution (10 mL) of maloic acid (0.10 g, 1 mmol) were added. The pH value was adjusted to 6 with $NH_3 \cdot H_2O$. The green mixture was placed in Teflon-lined stainless reactor and heated at 160 °C for 5-*d*. Green crystals of **1** were obtained (0.08 g, 36% based on Ni). Found: C, 16.17; H, 2.73; Cd, 25.92; Ni, 12.77%. Calc. for $C_6H_{12}CdNiO_{12}$: C, 16.11; H, 2.71; Cd, 25.13; Ni, 13.12%. IR (KBr, cm^{-1}): 3478, 3399 (ν_{O-H}); 2913 (ν_{C-H}); 1608, 1571 ($\nu_{as-COO-}$); 1457, 1395 (ν_{s-COO-}); 1272, 1179 ($\nu_{C-C,\ C-O}$); 740 (ν_{Ni-O}); 582 (ν_{Cd-O}).

2.2.2. Preparation of $[NiZn_2(Hcit)_2(H_2O)_2]_n$ **2**:

Citric acid (0.21 g, 1 mmol) were dissolved in deioned water (10 mL). Under constant stirring, $ZnSO_4 \cdot 7H_2O$ (0.29 g, 1 mmol) and $NiCl_2 \cdot 6H_2O$ (0.12 g, 0.5 mmol) in water (10 mL) were added. The pH value was adjusted to 6 with 1 M HCl. The color was green. The mixture was placed in Teflon-lined stainless reactor and heated at 140 °C for 5-*d*. Green crystals of **2** were obtained (0.13 g, 43% based on Ni). Found: C, 23.79; H, 2.35; Zn, 21.09; Ni, 10.07%. Calc. for $C_{12}H_{14}Zn_2NiO_{16}$: C, 23.88; H, 2.34; Zn, 21.66; Ni, 9.72%. IR (KBr, cm^{-1}): 3480, 3275 (ν_{O-H}); 2963 (ν_{C-H}); 1586, 1556, 1543($\nu_{as-COO-}$); 1426, 1400 (ν_{s-COO-}); 1137, 1082, 1076 ($\nu_{C-C,\ C-O}$); 681 (ν_{Ni-O}); 441 (ν_{Zn-O}).

2.2.3. Preparation of $[CoCd_2(Hcit)_2(H_2O)_2]_n$ **3**:

The preparation of **3** is the same to that of **2**. With the same ratios, the reagents were changed to $CdCl_2 \cdot 2.5H_2O$ and $CoCl_2 \cdot 6H_2O$. Purple crystals of **3** were obtained (0.11 g, 32% based on Co). Found: C, 20.72; H, 2.04; Cd, 31.25; Co, 8.71%. Calc. for $C_{12}H_{14}Cd_2CoO_{16}$: C, 20.65; H, 2.02; Cd, 32.21; Co, 8.44%. IR (KBr, cm^{-1}): 3478, 3390 (ν_{O-H}); 2977, (ν_{C-H}); 1588, 1553($\nu_{as-COO-}$); 1430, 1401 (ν_{s-COO-}); 1140, 1089, 1072 ($\nu_{C-C,\ C-O}$); 634 (ν_{Co-O}); 538 (ν_{Cd-O}).

2.2.4. Preparation of $[CoZn_2(Hcit)_2(H_2O)_2]_n$ **4**:

The preparation of **4** is the same to that of **2**. With the same ratios, the reagents were changed to $ZnSO_4 \cdot 7H_2O$ and $CoCl_2 \cdot 6H_2O$. Dark red crystals of **4** were obtained. (0.09 g, 36% based on Co). Found: C, 23.78; H, 2.35; Co, 9.02; Zn, 22.23%. Calc. for $C_{12}H_{14}Co_3O_{16}$: C, 23.87; H, 2.34; Co, 9.76; Zn, 21.65%. IR (KBr, cm^{-1}): 3500 (ν_{O-H}); 2929, (ν_{C-H}); 1607, 1588($\nu_{as-COO-}$); 1426, 1404 (ν_{s-COO-}); 1139, 1085, 1070 ($\nu_{C-C,\ C-O}$); 633 (ν_{Co-O}); 475 (ν_{Zn-O}).

2.3. Determination of crystal structure

X-ray diffraction data of the complexes were carried out on the Bruker Smart 1000 APEX II diffractometer equipment with graphite-monochromated Mo-$K\alpha$ radiation (λ=0.71073 Å) at 293(2) K and empirical absorption correction was applied. The structures were solved by the direct method and refined by full matrix least-squares method on F^2. All the structural calculations were taken out with the SHELXL-97 crystallographic software package [40,41]. Further details of X-ray structural analyses are given in Table 1. Selected bond lengths and angles are listed in the supplementary materials (Table S1).

3. Results and discussion

3.1. Structural descriptions of the polymers

3.1.1. Structural description of $[NiCd(mal)_2(H_2O)_2]_n \cdot 2nH_2O$ **1**

X-ray single-crystal structural analysis indicates that the asymmetric unit of **1** consists of one Cd(II) ion with an occupancy of 0.5, one Ni(II) ion with an occupancy of 0.5, one mal^{2-} group, one coordinated water and one lattice water molecule (Fig. 1). In the structure, Ni(II) ion is six-coordinated in a slightly distorted octahedral geometry with four O-atoms from two mal^{2-} groups and two O-atoms from two coordinated water molecules. The Cd(II) ion is six-coordinated by six O-atoms from four mal^{2-} groups leading to a CdO_6 near-octahedral coordination surrounding. The bond lengths of Ni–O are in the range of 2.046(2)–2.082(2) Å and those of Cd–O are 2.250(2)–2.574(2) Å. In the structure, the mal^{2-} group bridges two Cd(II) ions and one Ni(II) ion with chelate and syn-anti fashions (Fig. S1).

Cd(II) ions are linked by mal^{2-} groups forming a regular Cd_6-ring structure (Fig. 2). The Cd_6-ring structure is connected with six adjacent Cd_6-rings by co-corner forming a regular layer structure in the *ab* plane (Fig. S2).

The Cd(II) and Ni(II) ions are linked by mal^{2-} groups forming a 1D –Cd–Ni–Cd–Ni– chain along the *c*-axis (Fig. S3), which link the Cd(II) ions in the adjacent layers by mal^{2-} groups. Thus, polymer **1**

Table 1
Crystal data for **1–4.**

Complex	1	2	3	4
Empirical formula	$C_6H_{12}CdNiO_{12}$	$C_{12}H_{14}Zn_2NiO_{16}$	$C_{12}H_{14}Cd_2CoO_{16}$	$C_{12}H_{14}Zn_2CoO_{16}$
Formula weight	447.27	603.68	697.96	603.90
Crystal system	Trigonal	Triclinic	Monoclinic	Monoclinic
Space group	$R\bar{3}c$	$P\bar{1}$	$P2_1/c$	$P2_1/c$
a/Å, α/(°)	16.9701(9), 90	6.4769(10), 85.495(2)	6.0803(6), 90	6.1519(10), 90
b/Å, β/(°)	16.9701(9), 90	7.2236(12), 77.594(2)	15.0120(14),101.6600(10)	14.589(2), 102.728(2)
c/Å, γ/(°)	24.164(3), 120	9.6790(16), 81.213(2)	9.6888(9), 90	9.5883(15), 90
V/Å^3	6026.5(8)	436.59(12)	866.12(14)	839.4(2)
$D_{cal.}$/g · cm^{-3}, Z	2.218, 18	2.296, 1	2.676, 2	2.389, 2
Absorption coefficient/mm^{-1}	3.051	3.884	3.472	3.907
F(0 0 0)	3960	302	674	602
Reflections collected/unique	8095/1160 R_{int}=0.0226	2181/1520 R_{int}=0.0107	4254/528 R_{int}=0.0155	4137/1487 R_{int}=0.0293
Data/restraints/parameters	1160/0/98	1520/0/142	1528/0/142	1487/1/146
Goodness-of-fit on F^2	1.073	1.085	1.106	1.049
R_1, wR_2 ($I > 2\sigma(I)$)	0.0279, 0.0760	0.0295, 0.0765	0.0263, 0.0651	0.0289, 0.0718
R_1, wR_2 (all data)	0.0286, 0.0766	0.0331, 0.0782	0.0274, 0.0657	0.0346, 0.0745
Largest diff. peak and hole/e · Å^{-3}	1.432 and −0.726	0.581 and −0.704	0.724 and −0.680	0.465 and −0.647

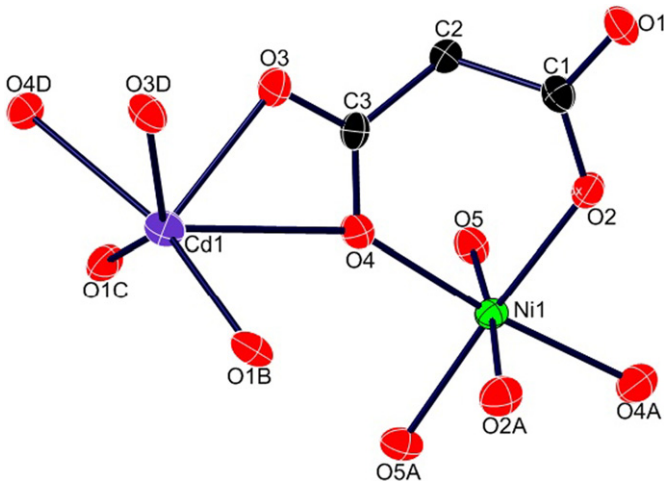

Fig. 1. Constructed unit of **1**.

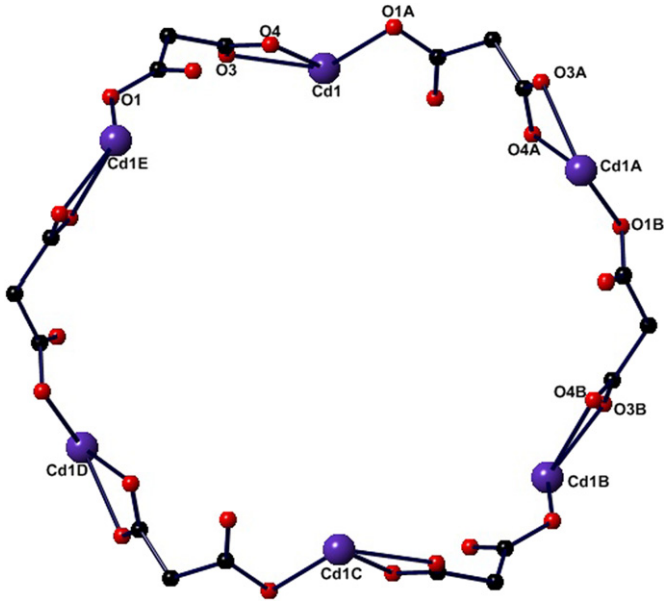

Fig. 2. Cd_6-ring structure in **1**.

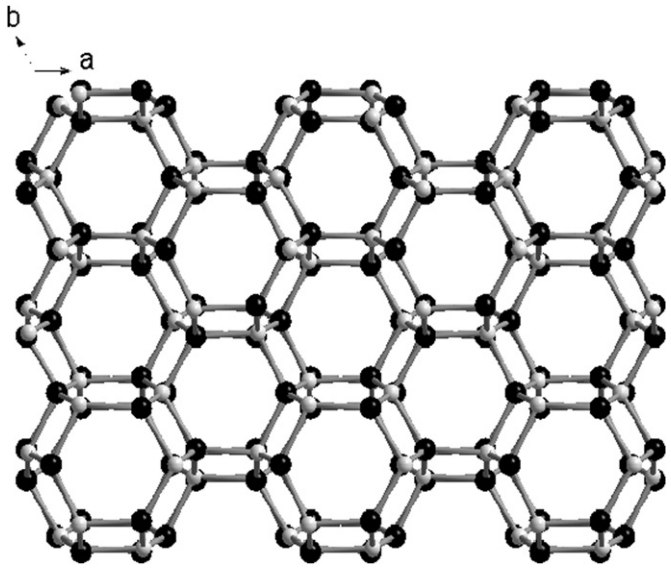

Fig. 3. Two-nodal (4,4)-connected $(4^2.6^4)_2$ topology of **1**.

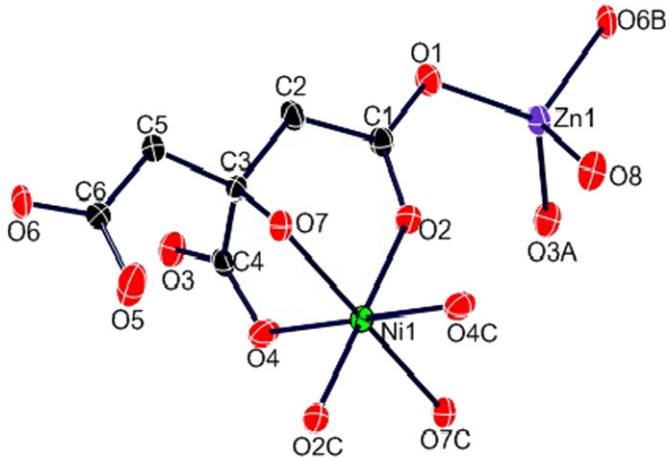

Fig. 4. Constructed unit of **2**.

is linked into a 3D structure (Fig. S4). In this 3D framework, both Ni(II) and Cd(II) ions serve as the 4-connected nodes. As a result, the overall structure of **1** can be assigned to an unusual two-nodal (4,4)-connected topology with the point symbol of $(4^2.6^4)_2$ whose topological type is SOD (Fig. 3). Drawing the polyhedron figure (CdO_6 and NiO_6 are octahedrons), there are regular hexagonal holes (Fig. S5). The lattice water molecules are joined in the formation of hydrogen bonds, which stabilize the structure. The percent unit cell volume occupied by lattice water molecules is 9.1% by the calculation of PLATON software.

3.1.2. *Structural description of* $[NiZn_2(Hcit)_2(H_2O)_2]_n$ **2**

X-ray single-crystal structural analysis indicates that the asymmetric unit of **2** includes one Zn(II) ion, one Ni(II) ion with an occupancy of 0.5 and special coordinates (0.5, 1.0, and 0.5), one $Hcit^{3-}$ group and one coordinated water molecule (Fig. 4). The Zn(II) ion is four-coordinated in a slightly distorted tetrahedral geometry with three carboxylate O-atoms from three $Hcit^{3-}$ groups and one O-atom from water molecule. The Ni(II) center has a slightly distorted octahedral geometry with equatorial plane provided by four carboxylate O-atoms and two hydroxyl O-atoms occupied the axial positions. The bond lengths of Zn–O are within 1.952(3)–2.008(4) Å and those of Ni–O are 2.044(3)–2.063(3) Å. The $Hcit^{3-}$ group bridges three Zn(II) ions and one Ni(II) ion with monodentate and syn-anti fashions (Fig. S6).

In the structure, the Zn(II) ions are linked by $Hcit^{3-}$ groups with bridging fashion into a 1D ladder-like chain along the *a*-axis (Fig. S7). The adjacent 1D chains are connected by the Ni(II) ions along the *c*-axis resulting in the 2D layer in the *ac* plane (Fig. S8). In this 2D layer structure, each Zn(II) and each $Hcit^{3-}$ ligand serve as the 3- and 4-connected nodes, respectively. As a result, the overall structure of **2** can be assigned to an unusual two-nodal (3,4)-connected topology with the point symbol of $(4^2.6)(4^2.6^3.8)$ whose topological type is 3,4L83 (1D_2D.ttd) (Fig. 5). The adjacent 2D layers are connected by the hydrogen bonds (O7–H…O1, 3.439 Å) between carboxyl and hydroxyl groups (Fig. S9), so polymer **2** is connected to a 3D supramolecular architecture.

3.1.3. *Structural description of* $[CoCd_2(Hcit)_2(H_2O)_2]_n$ **3**

The asymmetric unit of **3** consists of one Cd(II) ion, one Co(II) ion with an occupancy of 0.5 and special coordinates (0.5, 0.5, and 0.5), one $Hcit^{3-}$ group and one coordinated water molecule

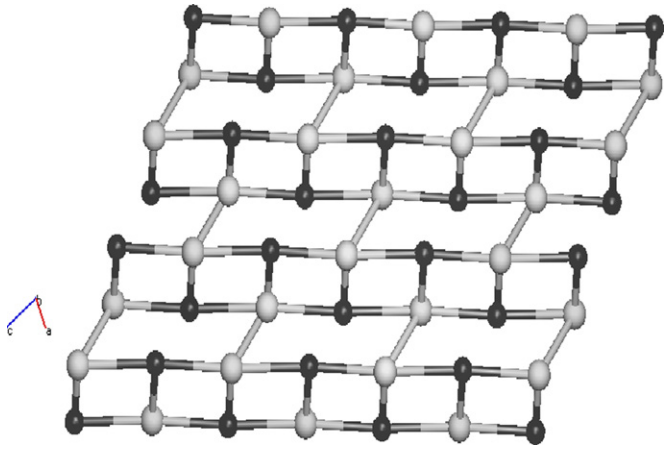

Fig. 5. Two-nodal (3,4)-connected ($4^2.6$) ($4^2.6^3.8$) topology of **2**.

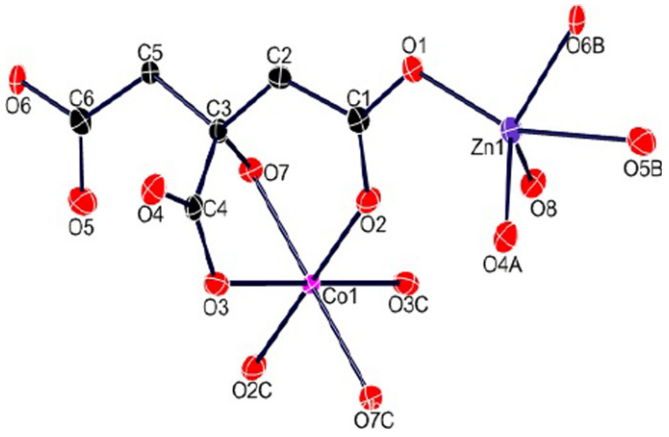

Fig. 7. Constructed unit of **4**.

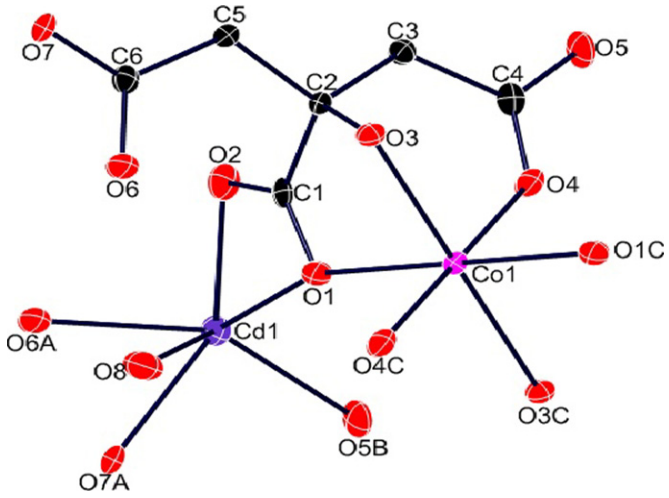

Fig. 6. Constructed unit of **3**.

(Fig. 6). The Cd(II) center is surrounded by a near octahedral environment of five carboxylate O-atoms from three $Hcit^{3-}$ groups and one O-atom from water molecule. The Co(II) center is in a slightly distorted octahedral geometry with six O-atoms from two $Hcit^{3-}$ groups. The bond lengths of Cd–O and Co–O are within 2.164(3)–2.635(2) Å and 2.081(2)–2.134(2) Å, respectively. The $Hcit^{3-}$ group bridges three Cd(II) ions and one Co(II) ion with chelate and syn-anti fashions (Fig. S10).

$Hcit^{3-}$ groups bridge Cd(II) ions to form a 1D ladder-like chain along the *a*-axis (Fig. S11). The adjacent 1D chains are connected by Co(II) ions along the *c*-axis resulting in the 2D layer structure in the *ac* plane (Fig. S12). The topologic structure of **3** is the same to **2**. The 3D supramolecular architecture of **3** is constructed by the hydrogen bonds (O3–H…O7, 2.684 Å) between carboxyl and hydroxyl groups (Fig. S13).

3.1.4. *Structural description of $[CoZn_2(Hcit)_2(H_2O)_2]_n$* **4**

Structural analysis indicates that the asymmetric unit of **4** consists of one Zn(II) ion, one Co(II) ion with an occupancy of 0.5 and special coordinates (1.0, 1.0, and 0.5), one $Hcit^{3-}$ group and one coordinated water molecule (Fig. 7). The Zn(II) ion is five-coordinated in a distorted square-pyramidal geometry all by O-atoms, four of which are from three $Hcit^{3-}$ groups and the other is the water molecule. The Co(II) ion is six-coordinated in a slightly distorted octahedral environment by six O-atoms from two $Hcit^{3-}$ groups. The bond lengths of Zn–O range from 1.973(2) to 2.306(3) Å and those of Co–O are within 2.051(2)–2.122(2) Å. The $Hcit^{3-}$ group bridges three Zn(II) ions and one Co(II) ion with chelate and syn-anti fashions (Fig. S14).

In the crystal, the Zn(II) ions are linked by $Hcit^{3-}$ groups forming a 1D ladder-like chain along the *a*-axis (Fig. S15). The Co(II) ions connected the adjacent ladder-like chains along the *c*-axis to form a 2D layer (Fig. S16). The topologic structure of **4** is the same to **2**. The adjacent layers are linked by the hydrogen bonds (O7–H…O6, 2.670 Å) between hydroxyl and carboxyl groups along the *b*-axis (Fig. S17). As a result a 3D supramolecular structure is formed for **4**.

From the structures of four polymers, we can see that they are all *M*–*M*′ heterometallic polymers (*M*=Ni/Co, *M*′=Cd/Zn) bridged by flexible carboxylate groups. The **1** is 3D structure bridged by mal^{2-} groups, while **2**–**4** are 2D structure bridged by $Hcit^{3-}$ groups with the same topologic structure. Although the $Hcit^{3-}$ groups in **2**–**4** all linked three *M*′ ions and one *M* ion, the coordination fashions are different in the polymers.

3.2. *The XRD and TG analysis*

The X-ray powder diffraction patterns of four complexes are consistent with the simulated those on the basis of the single-crystal structure data (Figs. S18 and S19), respectively. The diffraction peaks on both patterns correspond well in position, indicating the phase purity of the samples. The difference in reaction intensities between the simulated and experimental patterns was due to the variation in crystal orientation for the power samples. The thermal stability of the complexes was measured by TG analysis (Fig. S20). The results show that the mass of **1** is unstable because of the existence of the lattice water and the mass of **2**–**4** remain stable.

3.3. *The assignment of UV–Vis absorption spectra of polymers*

There are five absorption bands in the UV–Vis absorption spectrum of **1** (Fig. S21), which indicates that there are transitions of charges in the outer shell under UV–Vis light inducement. The band (λ_{max}=252 nm) is assigned to the ligand-to-ligand charge transition (LLCT) and the band (λ_{max}=332 nm) is assigned to ligand–metal charge transition (LMCT and MLCT). The bands at 393, 640, and 1077 nm are assigned to the d→d* transitions of Ni(II) ions ($^3A_{2g}\rightarrow{}^3T_{1g}(P)$, $^3A_{2g}\rightarrow{}^3T_{1g}(F)$, and $^3A_{2g}\rightarrow{}^3T_{2g}$).

The absorption bands in the UV–Vis spectrum of **2** (Fig. S22) are similar to those of **1**. The band at 253 nm can be assigned to the LLCT and the band at 301 nm is the LMCT and MLCT.

The bands (λ_{max}=407, 718, and 1168 nm) are the d→d* transitions of Ni(II) ions ($^3A_{2g}\rightarrow{}^3T_{1g}$(P), $^3A_{2g}\rightarrow{}^3T_{1g}$(F), $^3A_{2g}\rightarrow{}^3T_{2g}$).

There are five absorption bands in the UV–Vis spectrum of **3** (Fig. S23), in which the band (λ_{max}=254 nm) is attributed to LLCT and the band at 343 nm is the LMCT and MLCT. The bands at 444, 518, and 1124 nm are attributed to the d→d* transitions of Co(II) ions, i.e., $^4T_{1g}\rightarrow{}^4A_{2g}$, $^4T_{1g}\rightarrow{}^4T_{1g}$ and $^4T_{1g}\rightarrow{}^4T_{2g}$.

The UV–Vis spectrum of **4** (Fig. S24) is similar to those of **3**, in which the band at 254 nm is the LLCT and the band at 289 nm is the LMCT and MLCT, and the others at 496, 581 and 1126 nm are the d→d* transitions of Co(II) ions, i.e., $^4T_{1g}\rightarrow{}^4A_{2g}$, $^4T_{1g}\rightarrow{}^4T_{1g}$ and $^4T_{1g}\rightarrow{}^4T_{2g}$.

3.4. The analysis and assignment of surface photovoltage spectroscopy (SPS) of polymers

Seen from the UV–Vis absorption spectra of four polymers, there are good light absorptions including the LLCT, LMCT, MLCT and d→d* transitions. These absorption bands nearly covered the entire UV–Vis region and the energies of these bands are in the bandgap energies of semiconductor, so they can be seen as broad semiconductors. In this paper, energy-band theory of semiconductor and crystal field theory were combined to analyze and assign the SPS, i.e., 2*s*2*p* orbitals of coordinated atoms form valence band; 4*s*4*p* orbitals of central metal ions form conduction band and *d* orbitals of the metal ions are considered as impurities.

There are wide photovoltage response bands within 300–800 nm in the SPS of **1**, which indicates that there are separations and transitions of surface charges to form electron–holes pairs under UV–Vis light inducement. The surface photovoltage difference is formed by the directional movements of electron–holes pairs, thus, there are response bands in the SPS, which indicates it possesses photoelectric conversion properties. The response bands were treated by Origin 7.0 and four bands were obtained (λ_{max}=339, 370, 430, 701 nm, Fig. 8). According to the energy–band theory of semiconductor, the bands at 339 and 370 nm are assigned to the band–band transitions from valance bands to conduction bands, i.e., Cd–O and O–Ni transitions. The response bands (λ_{max}=430, 701 nm) are assigned to the impurity transitions from d orbitals of Ni(II) ions, which are corresponded to the d→d* transitions of Ni(II) ions ($^3A_{2g}\rightarrow{}^3T_{1g}$(P)and $^3A_{2g}\rightarrow{}^3T_{1g}$(F)).

The SPS of **2** (Fig. 9) is similar to that of **1**, in which there are four photovoltage response bands within 300–800 nm after the treatment of Origin 7.0. The response bands at 346 and 381 nm

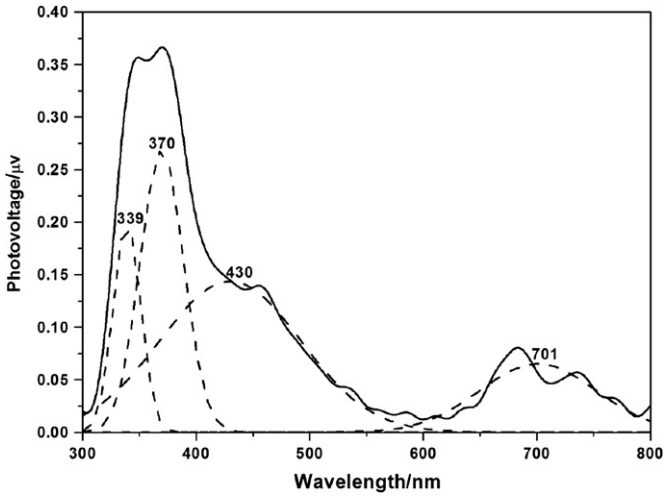

Fig. 8. SPS of **1**.

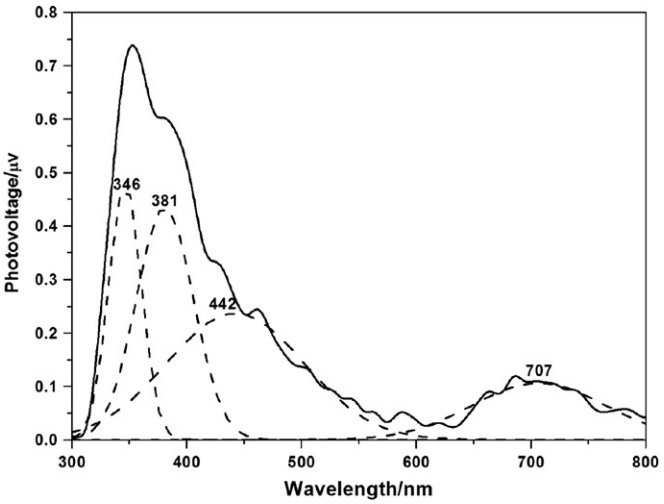

Fig. 9. SPS of **2**.

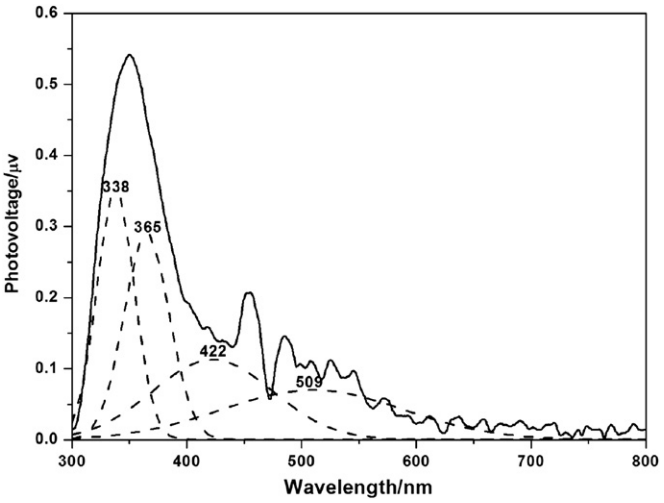

Fig. 10. SPS of **3**.

can be assigned to the band–band transitions (Zn–O and O–Ni). The bands (λ_{max}=442, 707 nm) are assigned to the impurity transitions corresponding to the d→d* transitions of Ni(II) ions, $^3A_{2g}\rightarrow{}^3T_{1g}$(P) and $^3A_{2g}\rightarrow{}^3T_{1g}$(F).

There are also four response bands in the SPS of **3** (Fig. 10), but the wavelength range of the response bands is narrower than that of **1** and **2**. The bands (λ_{max}=338, 365 nm) can be attributed to the band–band transitions, i.e., Cd–O and O–Co. The bands at 422, and 509 nm are the impurity transitions corresponding to the d→d* transitions of Co(II) ions ($^4T_{1g}\rightarrow{}^4A_{2g}$, and $^4T_{1g}\rightarrow{}^4T_{1g}$).

The SPS of **4** (Fig. 11) is similar to that of **3**, which includes four photovoltage response bands (λ_{max}=347, 382, 436, and 532 nm). The former two bands can be attributed to the band–band transitions, i.e., Zn–O and O–Co. The latter two response bands can be attributed to the impurity transitions corresponding to the d→d* transitions of Co(II) ions, i.e., $^4T_{1g}\rightarrow{}^4A_{2g}$ and $^4T_{1g}\rightarrow{}^4T_{1g}$.

3.5. The comparative analysis of surface photoelectric properties of heterometallic polymers

There are good corresponding relationships between SPS and UV–Vis absorption spectra of four heterometallic polymers. The band–band transitions in the SPS are corresponded to the charge transitions in the UV–Vis spectra and the impurity transitions are

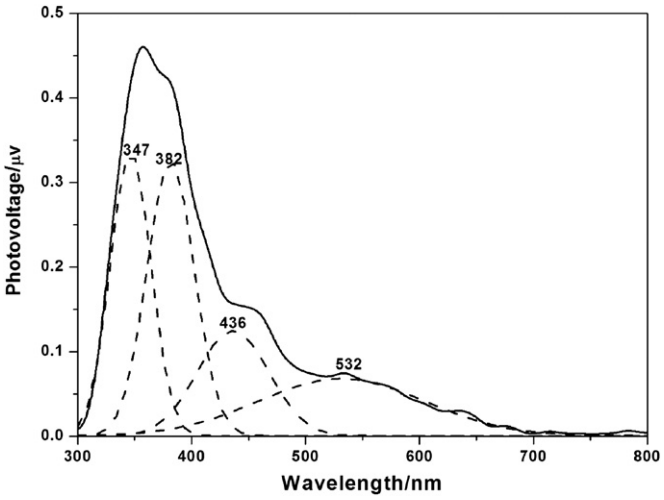

Fig. 11. SPS of **4**.

corresponded to the d→d* transitions. The LLCT transition at about 250 nm and the d→d* transition at 1100 nm in the UV–Vis absorption spectra cannot be observed in the SPS because of the region of SPS apparatus (300∼800 nm).

The SPS of four polymers, Ni–Cd, Ni–Zn, Co–Cd, Co–Zn were compared and they were also compared with the SPS of corresponding monometallic complexes. (The SPS of $[Ni(H_2O)_6]\cdot H_2btec$ and $[Zn(NO_2C_6H_4CO_2)_2(H_2O)(phen)]$ were detected and the SPS of $[Cd_3(Hcit)_2(H_2O)_2]_n$ [38] and Co–btec complexes [42] were taken as references. The SPS and assignments of these complexes were listed in the Section 5 of supplementary materials.) We can find:

(i). There are photovolatge response bands in the range of 300–800 nm in the SPS for four heterometallic coordination polymers, which indicates that the surface electrons are separated and transferred forming electron–holes pairs under UV–Vis light inducement. The electron–holes pairs move directionally under the built-in electric field resulting in the change of surface photovoltage, i.e., possessing photoelectric conversion properties.

(ii). Since M'(II) ions (Zn or Cd) were introduced in the four polymers, there are band–band transitions of M'–O besides O–Co and O–Ni by the d^{10} electron configuration.

(iii). The range of response bands in **1** and **3** is obviously broader than that of $[Cd_3(Hcit)_2(H_2O)_2]_n$ complex (300–400 nm, Fig. S25). Similarly, the range of response bands in **2** and **4** are obviously wider than that of $[Zn(NO_2C_6H_4CO_2)_2(H_2O)(phen)]$ complex (Fig. S27). The reasons for these are the introductions of M(II) ions (Ni or Co).

(iv). The range of response bands in **1** and **2** (300–800 nm) are obviously broader than that of $[Ni(H_2O)_6]\cdot H_2btec$ complex (300–650 nm, Fig. S28). The range of response bands in **3** and **4** (300–650 nm) are broader than that of Co–btec complexes (300–550 nm, Fig. S29). All of which are by the reason of the introduction of M'(II) ions (Zn or Cd).

(v). Compared with the SPS of four polymers, the species of introduced transition metal M(II) ions (Ni or Co) affect the number and position of impurity transition bands obviously when the M' metals are the same, because the impurity transition bands are different. If the M(II) ions (Ni or Co) are the same and M' ions are different, the response bands in the SPS are the same basically with a few differences in the extent of broadening.

4. Conclusions

Four new heterometallic coordination polymers (Ni–Cd, Ni–Zn, Co–Cd, Co–Zn) were synthesized and characterized, in particularly, the photoelectric properties of heterometallic polymers were discussed by SPS. There are two species of response bands in the SPS of four polymers, i.e., band–band transition and impurity transition. From the comparisons of SPS for four polymers and SPS for corresponded monometallic complexes, the range of response bands in the heterometallic polymers is broadened obviously than that of the monometallic complexes because of the introduction of other transition metal ions. The different species of heterometallic ions affect the position, width and number of response bands in the SPS. It is obvious that heterometallic coordination polymers broaden the response range of UV and Visible light, which may provide an important reference for the exploiting of photoelectric conversion materials with wide light response range.

Supplementary data: CCDC <791699, 791700, 791701 and 791702.> contain the supplementary crystallographic data for **1–4**. These data can be obtained free of charge via http://www.ccdc.cam.ac.uk/conts/retrieving.html, or from the Cambridge Crystallographic Data Centre, 12 Union Road, Cambridge CB2 1EZ, UK; fax: (+44) 1223-336-033; or e-mail: deposit@ccdc.cam.ac.uk. The supplementary structural figures, XRD spectra, TG curves, UV–Vis spectra and SPS of monometallic complexes are presented in the Supplementary Information.

Acknowledgments

The research was supported by the National Natural Science Foundation of China (20571037) and the Educational Foundation of Liaoning Province in China (2007T092).

Appendix A. Supplementary material

Supplementary data associated with this article can be found in the online version at doi:10.1016/j.jssc.2011.03.046.

References

[1] Y.G. Huang, F.L. Jiang, M.C. Hong, Coord. Chem. Rev. 253 (2009) 2814–2834.
[2] H. He, G.J. Cao, S.T. Zheng, G.Y. Yang, J. Am. Chem. Soc. 131 (2009) 15588–15589.
[3] I.P.C. Liu, C.H. Chen, C.F. Chen, G.H. Lee, S.M. Peng, Chem. Commun. (2009) 577–579.
[4] M. Zhang, T. Sheng, X. Wang, S. Hu, R. Fu, J. Chen, Y. He, Z. Qin, C. Shen, X. Wu, Cryst. Eng. Comm 12 (2010) 73–76.
[5] G. Agustí, M.C. Muñoz, A.B. Gaspar, J.A. Real, Inorg. Chem. 48 (2009) 3371–3381.
[6] V.M. Nikitina, O.V. Nesterova, V.N. Kokozay, E.A. Goreshnik, J. Jezierska, Polyhedron 27 (2008) 2426–2430.
[7] V.V. Semenaka, O.V. Nesterova, V.N. Kokozay, R.I. Zybatyuk, O.V. Shishkin, R. Boča, D.V. Shevchenko, P. Huang, S. Styring, Dalton Trans. 39 (2010) 2344–2349.
[8] X.L. Wang, B.K. Chen, G.C. Liu, H.Y. Lin, H.L. Hu, J. Organometal. Chem 695 (2010) 827–832.
[9] Y.X. Chi, S.Y. Niu, J. Jin, R. Wang, Y. Li, Dalton Trans. (2009) 7653–7659.
[10] S. Albedyhl, D. Schnieders, A. Jancsó, T. Gajda, B. Krebs, Eur. J. Inorg. Chem. (2002) 1400–1409.
[11] Y.Z. Zhou, J. Liu, Inorg. Chem. Commun. 12 (2009) 243–245.
[12] Y. Song, P. Zhang, X.M. Ren, X.F. Shen, Y.Z. Li, X.Z. You, J. Am. Chem. Soc. 127 (2005) 3708–3709.
[13] G.C. Guo, M.S. Wang, L.Z. Cai, J.S. Huang, Eur. J. Inorg. Chem. (2010) 2826–2835.
[14] Y.X. Chi, S.Y. Niu, Z.L. Wang, J. Jin, Eur. J. Inorg. Chem. (2008) 2336–2343.
[15] L.P. Engelhardt, C.A. Muryn, R.G. Pritchard, G.A. Timco, F. Tuna, R.E.P. Winpenny, Angew. Chem. Int. Ed. 47 (2008) 924–927.
[16] G.A. Timco, E.J.L. McInnes, R.G. Pritchard, F. Tuna, R.E.P. Winpenny, Angew. Chem. Int. Ed. 47 (2008) 9681–9684.

[17] J. Jin, S. Niu, Q. Han, Y. Chi, New J. Chem. 34 (2010) 1176–1183.
[18] Y.X. Chi, S.Y. Niu, J. Jin, Inorg. Chim. Acta 362 (2009) 3821–3828.
[19] H.R. Wen, Y.Z. Tang, C.M. Liu, J.L. Chen, C.L. Yu, Inorg. Chem. 48 (2009) 10177–10185.
[20] D. Zhang, H. Wang, Y. Chen, Z.H. Ni, L. Tian, J. Jiang, Inorg. Chem. 48 (2009) 11215–11225.
[21] Y. Bai, W.L. Shang, D.B. Dang, H. Gao, X.F. Niu, Y.F. Guan, Inorg. Chem. Commun. 11 (2008) 1470–1473.
[22] M. Andruh, J.P. Costes, C. Diaz, S. Gao, Inorg. Chem. 48 (2009) 3342–3359.
[23] L. Kronik, Y. Shapira, Surf. Sci. Rep. 37 (1999) 1–206.
[24] L. Jing, X. Sun, J. Shang, W. Cai, Z. Xu, Y. Du, H. Fu, Sol. Energy Mater. Sol. Cells 79 (2003) 133–151.
[25] L. Kronik, Y. Shapira, Surf. Interface Anal. 31 (2001) 954–965.
[26] L.S. Li, Q.X. Jia, A.D.Q. Li, Chem. Mater. 14 (2002) 1159–1165.
[27] A.D.Q. Li, L.S. Li, J. Phys. Chem. B 108 (2004) 12842–12850.
[28] Y. Lin, D. Wang, Q. Zhao, M. Yang., Q. Zhang, J. Phys. Chem. B 108 (2004) 3202–3206.
[29] Q. Zhang, D. Wang, J. Xu, J. Cao, J. Sun, M. Wang, Mater. Chem. Phys. 82 (2003) 525–528.
[30] Y. Zhang, H. Zhang, Y. Wang, W.F. Zhang, J. Phys. Chem. C 112 (2008) 8553–8557.
[31] M. Yu, W. Zhang, Y. Fan, W. Jian, G. Liu, J. Phys. Org. Chem. 20 (2007) 229–235.
[32] E.J. Sun, Z.Y. Sun, M. Yuan, D. Wang, T.S. Shi, Dyes and Pigments 81 (2009) 124–130.
[33] E. Sun, X. Cheng, D. Wang, X. Tang, S. Yu, T. Shi, Solid State Sci. 9 (2007) 1061–1068.
[34] L. Zhang, S.Y. Niu, J. Jin, L.P. Sun, G.D. Yang, L. Ye, Inorg. Chim. Acta 362 (2009) 1448–1454.
[35] L.P. Sun, S.Y. Niu, J. Jin, L. Zhang, Eur. J. Inorg. Chem. (2007) 3845–3852.
[36] L.P. Sun, S.Y. Niu, J. Jin, G.D. Yang, L. Ye, Inorg. Chem. Commun. 9 (2006) 679–682.
[37] B. Li, L. Bi, W. Li, L. Wu, J. Solid State Chem. 181 (2008) 3337–3343.
[38] L. Li, J. Jin, Z. Shi, L. Zhao, J. Liu, Y. Xing, S. Niu, Inorg. Chim. Acta 363 (2010) 748–754.
[39] W. Chen, H.M. Yuan, J.Y. Wang, Z.Y. Liu, J.J. Xu, M. Yang, J.S. Chen, J. Am. Chem. Soc. 125 (2003) 9266–9267.
[40] G.M. Sheldrick, SHELXS–97, Program for Crystal Structure Solution, University of Göttingen, Germany, 1997.
[41] G.M. Sheldrick, SHELXL–97, Program for Structure Refinement, University of Göttingen, Germany, 1997.
[42] Z.F. Shi, J. Jin, L. Li, Y.H. Xing, S.Y. Niu, Acta Phys.-Chim. Sin. 25 (2009) 2011–2019.